ICA 2019 AACHEN

PROCEEDINGS of the
23rd International Congress on Acoustics

9 to 13 September 2019 in Aachen, Germany

Vibro-acoustic rendering methods to radiate a uniform sound field from a panel speaker

Jung-Han Woo[1,2]; Jeong-Guon Ih[1]

[1] Korea Advanced Institute of Science and Technology (KAIST), Daejeon, Korea

[2] Currently at Korea Institute of Machinery and Materials (KIMM), Daejeon, Korea

ABSTRACT

The sound radiated from the usual panel speaker employing the single point excitation is distorted due to the multi-modal response of the regular panel, or the effective range of radiation is limited to very low frequencies. Such problem can be alleviated if an array of actuators is used in the periphery of the panel to control the vibration response for the uniform radiation in a wide frequency range. To achieve the uniform acoustic field, the two inverse vibro-acoustic rendering techniques can be adopted: first, a vibration pattern composed of a virtual speaker and baffle is being created, and, second, the spatial distribution of the vibration is being controlled to radiate the desired sound. Each method is called indirect or direct method. Numerical simulations are conducted on a thin, simply-supported plate, for which the high frequency limit is 300 Hz. The indirect method results the rendering error of -20 dB and the direct method -50 dB. Two methods are afflicted with the instability, particularly in using the direct one. Regularization technique is used to overcome the ill-posedness, that yields the change of condition number from $O(10^{17})$ to $O(10^{4})$. Input gains are also reduced by 35 dB for both methods.

Keywords: Panel speaker, actuator array, vibro-acoustic rendering, vibro-acoustic inverse technique

1. INTRODUCTION

Audio systems embedded in various machines or devices often concerns about the acoustic power and low frequency contents because they are usually constrained in the spatial usage for a compact layout to have the aesthetic shape and geometric efficiency [1-4]. The generated sounds from them are usually distorted due to the multi-modal characteristic of the plate, and the radiation efficiency is low. To overcome such problems, a method of using an array of multiple actuators located at the periphery of a thin plate or surrounding the main actuator is proposed [5].

Two methods converting a panel into an effective sound radiator using the actuator array are considered: one is to create the circular speaker and tranquil baffle zones simultaneously, and the other is to specify the vibration distribution on a panel that can eventually realize the desired sound radiation. In this work, the characteristics of two inverse rendering methods are compared.

2. DIRECT & INDIRECT INVERSE RENDERING METHODS

2.1 Indirect inverse rendering method (IRM)

The vibration pattern composed of virtual speaker and baffle zones can be created to achieve the desired sound radiation. The created speaker and baffle can be considered as the virtual speaker system. Similar to the real loudspeaker, an in-phase back-and-forth piston motion with the amplitude v_{spk} is expected in the speaker zone. Ideally, there should be no phase difference within the speaker zone and no vibration at the baffle zone. In the steady state, the relation between the velocity responses at the

[1] jhwoo@kimm.re.kr
[2] J.G.Ih@kaist.ac.kr

M observation points on the plate and the excitation forces at the actuators is given by

$$[\mathbf{G}]_{M\times N}[\mathbf{e}]_{N\times 1}=[\mathbf{v}]_{M\times 1}, \tag{2}$$

where N is the number of actuators, $\mathbf{e}$ the input force vector at the actuator positions, $\mathbf{v}$ the velocity vector at the observation points on the plate, and $\mathbf{G}$ the transfer function between actuators and observation points [6]. A least-squares solution minimizing the error between the rendered vibration pattern and the created vibration field can be obtained by the Moore-Penrose inverse as follows:

$$\min\left\|\mathbf{v}_t-\hat{\mathbf{v}}\right\| \text{ subject to } \hat{\mathbf{v}}=\mathbf{G}\hat{\mathbf{e}}_1, \qquad [\hat{\mathbf{e}}_1]_{N\times 1}=[\mathbf{G}]^{\dagger}_{N\times M}[\mathbf{v}_t]_{M\times 1}=\left(\mathbf{G}^*\mathbf{G}\right)^{-1}\mathbf{G}^*\mathbf{v}_t. \tag{3, 4}$$

Here, $\hat{\mathbf{e}}_1$ means the estimated input force vectors obtained by applying the IRM, $\mathbf{v_t}$ the rendered vibration field, $\hat{\mathbf{v}}$ the generated vibration velocity field, ||…|| the Euclidean norm, and $\mathbf{G}^{\dagger}$, $\mathbf{G}^*$ indicate the pseudo inverse and the conjugate transpose of the matrix $\mathbf{G}$, respectively [6,7].

2.2 Direct inverse rendering method (DRM)

Another method for achieving the desired sound radiation can be thought of. The panel can be set into the vibration by the actuator array to directly radiate the desired sound pattern without imposing any constraint on the source vibration pattern. The complex gain for the input force of the actuator array is estimated from the direct inverse transfer relationship between the desired acoustic field and the actuator array. The input forces for control actuators can be obtained as

$$\min\left\|\mathbf{p}_t-\hat{\mathbf{p}}\right\| \text{ subject to } \hat{\mathbf{p}}=\mathbf{H}\hat{\mathbf{e}}_2, \qquad [\hat{\mathbf{e}}_2]_{N\times 1}=[\mathbf{H}]^{\dagger}_{N\times Q}[\mathbf{p}_t]_{M\times 1}=\left(\mathbf{H}^*\mathbf{H}\right)^{-1}\mathbf{H}^*\mathbf{p}_t. \tag{5,6}$$

Here, $\mathbf{H}$ indicates the Green's function between plate vibration and radiated sound pressure, Q the number of observation points in acoustic field, $\hat{\mathbf{e}}_2$ the estimated input force vector using the DRM, $\mathbf{p_t}$ the desired sound field, and $\hat{\mathbf{p}}$ the actually generated acoustic field.

3. COMPARISON OF THE TWO RENDERING METHODS

To test the two inverse rendering methods, a simply supported aluminum plate with a size of 700 mm x 400 mm x 2 mm is used. A total of 196 actuators are located near the plate edges in 10-mm uniform spacing to avoid the spatial aliasing. Vibration observation points are distributed at 2079 points in the panel, and the radiated sound field on a hemispherical surface are observed at 3751 points, which are 1 m away from the plate center. In this work, the error in the acoustic field, ε_p, to quantify the difference between desired and generated fields, and the input power, W_e, for generating the rendered vibration or acoustic field are defined as

$$\varepsilon_p=20\log_{10}\left(\int_q\left|(\hat{p}-p_t)/p_t\right|/Q\right), \quad W_e=20\log_{10}\left(\sum_{n=1}^{N}\left|\hat{e}/e_{ref}\right|\right). \tag{7,8}$$

3.1 Results of inverse rendering

To generate a uniform hemispherical sound radiation pattern, the condition $kR\ll 1$ should be satisfied. To adopt the IRM, a virtual speaker zone with a radius of 75 mm is predetermined on the plate center. The test result with IRM is illustrated in Fig. 1. One can see that the estimated error of the generated sound field increases with frequency in general except at 180 Hz, which approximately corresponds to the first longest bending wavelength matching the distance between speaker center and plate corner [5]. Created vibration magnitude and phase fulfilling the rendered sound radiation are shown in Fig. 2. When the DRM is used, the system ill-conditioning influences the created vibration field a lot. The average condition number of DRM is about 10^{17}, which means that the use of regularization is essential in solving the instability problem.

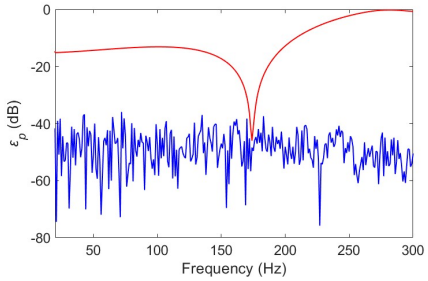

Figure 1 – The reconstruction error by using the two inverse rendering methods: ——, IRM; ——, DRM.

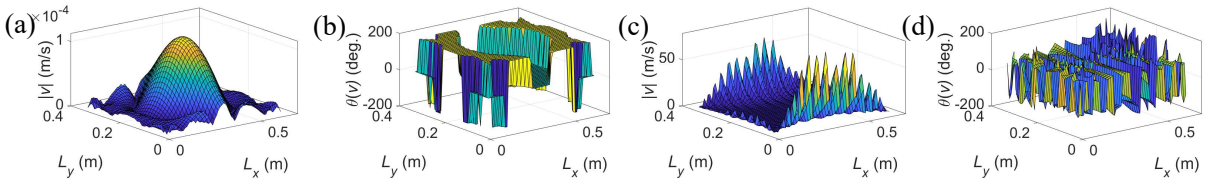

Figure 2 – Vibration field as virtual speaker and baffle at 160 Hz:

(a)(c) magnitude, (b)(d) phase; (a)(b) IRM, (c)(d) DRM.

3.2 Effect of regularization

Among various regularization techniques for obtaining the stable inverse solution of an ill-conditioned matrix [6-8], Tikhonov method [9] is employed modified separately for IRM and DRM. The cost functions for suppressing the instability in using the IRM and DRM, respectively, are composed of the error between rendered target fields, vibration velocity $\mathbf{v}_t$ or acoustic pressure $\mathbf{p}_t$, and reconstructed fields, $\mathbf{G}\hat{\mathbf{e}}_{1F}$ or $\mathbf{H}\hat{\mathbf{e}}_{2F}$, and the weighted input power. Here, $\hat{\mathbf{e}}_{1F}$ and $\hat{\mathbf{e}}_{2F}$ imply the regularized input force signal. In this work, the optimal regularization parameter β is obtained by using the L-curve method [10]. To consider the noise-contaminated condition, the normally distributed random noise is added to the initial rendered field varying the SN ratio of the target field. Figure 3 exhibits the simulation results illustrating the required input energy for the actuators versus the reconstruction error of the acoustic field. One can find that the DRM results are strongly influenced by the included noise. This coincides with the fact that the condition of the system using the DRM is much more ill-posed than that of the IRM. Figures 4 and 5 compare the created vibration field and the estimated input gains of actuators at 160 Hz with the severely contaminated field condition with noise. After regularization, the initial condition number $6.6\text{x}10^{16}$ is reduced to $1.1\text{x}10^{5}$, which is a similar value with the system of IRM. One can find that the input gains of actuators are much reduced after the regularization, in particular, the input gain magnitude of DRM is reduced by about 35 dB.

4. Conclusions

To radiate the desired sound using actuator array located at the periphery of a thin plate surface, two possible rendering methods are considered to compare their capability in radiating a uniform sound field. It is shown that the control by using DRM requires too large amount of input power. To overcome the ill-posed problem in the inverse rendering process, the regularization is adopted, which results in much reduced and stable input gains even under a highly contaminated signal condition. Decision on what method is to be used can be made by considering both the acceptable reconstruction error to be achieved and the input power needed for the control actuators for practical applications.

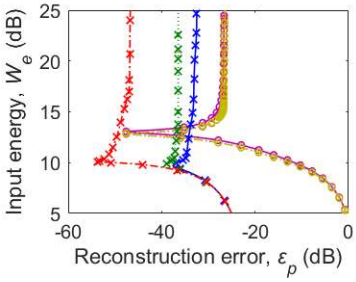

Figure 3 – Required input energy of the actuators related to the reconstruction error of the acoustic field (160 Hz): O, IRM; ✕ , DRM; ——, SNR=5 dB; ------, SNR=10 dB; -·-·-, SNR=20 dB.

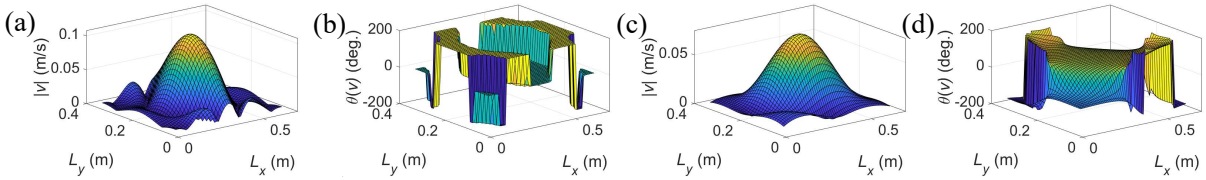

Figure 4 – Created vibration field on the plate after the regularization (160 Hz, SNR =10 dB):

(a)(c) magnitude, (b)(d) phase; (a)(b) IRM, (c)(d) DRM.

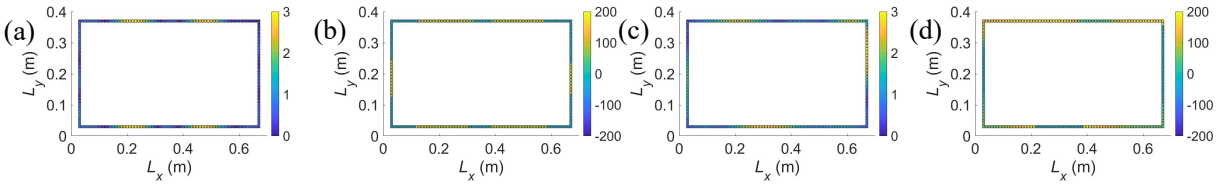

Figure 5 – Calculated input gains of actuators after the regularization (160 Hz, SNR =10 dB): (a)(c) magnitude, (b)(d) phase; (a)(b) IRM, (c)(d) DRM.

ACKNOWLEDGEMENTS

This work was partially supported by the BK21-Plus Project and the NRF grants (No. 2016K2A9A2A12003779 and No. 2017R1A2B4007133).

REFERENCES

1. Woodard S. Improvements of modal max high-fidelity piezoelectric audio device. NASA Tech Briefs. 2005; 36.
2. Harris N, Hawksford MOJ. The distributed-mode loudspeaker (DML) as a broad-band acoustic radiator. Proc. Audio Eng. Soc. 1997; 45: 1007.
3. Bai MR, Huang T. Development of panel loudspeaker system: design, evaluation and enhancement. J. Acoust. Soc. Am. 2001; 109: 2751-2761.
4. Feonic Plc. Magnetostrictive actuator. US Patent 8471432. 2013.
5. Woo JH, Ih JG. Generation of a virtual speaker and baffle on a thin plate controlled by an actuator array at the boundary. To appear at IEEE/ASME Trans. Mechatronics. 2019.
6. Bai M, Ih JG, Benesty J. Acoustic Array Systems: Theory, Implementation, and Application. Singapore: Wiley; 2013.
7. Kim BK, Ih JG. Design of an optimal wave-vector filter for enhancing the resolution of reconstructed source field by near-field acoustical holography (NAH). J. Acoust. Soc. Am. 2000; 107:3289-3297.
8. Williams EG. Regularization methods for near-field acoustical holography. J. Acoust. Soc. Am. 2001; 110:1976-1988.
9. Tikhonov AN, Arsenin VY. Solutions of Ill-Posed Problems. New York, USA: Wiley; 1977.
10. Hansen PC, O'Leary DP. The use of the L-curve in the regularization of discrete ill-posed problems. SIAM J. Sci. Comput. 1993; 14: 1487-1503.